View metadata, citation and similar papers at core.ac.uk
brought to you by CORE
provided by DigitalCommons@University of Nebraska

University of Nebraska - Lincoln
DigitalCommons@University of Nebraska - Lincoln

Xiao Cheng Zeng Publications | Published Research - Department of Chemistry

June 2008

Anisotropy of crystal-melt interfacial free energy of silicon by simulation

Pankaj A. Apte
University of Nebraska-Lincoln

Xiao Cheng Zeng
University of Nebraska-Lincoln, xzeng1@unl.edu

Follow this and additional works at: https://digitalcommons.unl.edu/chemzeng

Part of the Chemistry Commons

Apte, Pankaj A. and Zeng, Xiao Cheng, "Anisotropy of crystal-melt interfacial free energy of silicon by simulation" (2008). *Xiao Cheng Zeng Publications*. 82.
https://digitalcommons.unl.edu/chemzeng/82

This Article is brought to you for free and open access by the Published Research - Department of Chemistry at DigitalCommons@University of Nebraska - Lincoln. It has been accepted for inclusion in Xiao Cheng Zeng Publications by an authorized administrator of DigitalCommons@University of Nebraska - Lincoln.

Anisotropy of crystal-melt interfacial free energy of silicon by simulation

Pankaj A. Apte[a)] and X. C. Zeng[b)]
Department of Chemistry, University of Nebraska–Lincoln, Lincoln, Nebraska 68588, USA

(Received 19 March 2008; accepted 8 May 2008; published online 2 June 2008)

We extend the cleaving wall method to a nonpairwise additive potential. Using this method, we compute the anisotropy of crystal-melt interfacial free energy γ for Stillinger–Weber potential of silicon [F. H. Stillinger and T. A. Weber, Phys. Rev. B **31**, 5262 (1985)]. The calculated γ for (100), (111), and (110) orientations are 0.42 ± 0.02, 0.34 ± 0.02, and 0.35 ± 0.03 J/m^2, respectively. The anisotropy in γ we found is consistent with the experimental observation that Si(100)-melt interface develops (111) facets and also helps in explaining a higher undercooling observed for Si(111)-melt interface in Czochralski method. © *2008 American Institute of Physics*. [DOI: 10.1063/1.2937444]

Bulk crystalline silicon (about 95%) for the semiconductor industry is manufactured using Czochralski (CZ) method.[1] Certain features of CZ method are noteworthy. At a typical growth rate of $\sim 5 \times 10^{-5}$ m/s, an undercooling of about 5° exists at the Si(111)-melt interface, whereas for all other orientations, undercooling is only of the order of millidegrees.[1–3] It is also observed[2,4–6] that Si(111)-melt interface is smooth and sharp, while Si(100)-melt interface is rough and exhibits (111) facets. These observed phenomena depend crucially on underlying free energetics determined by crystal-melt interfacial energy γ and its anisotropy, which governs the kinetics and morphology of crystal growth.[7–9] Although a number of experimental[10–13] and computational[14,15] studies have attempted to obtain γ for silicon, the anisotropy of γ has not been obtained. In this letter, we present results on the anisotropy for Stillinger–Weber (SW) potential[16] of silicon using cleaving wall method.[17–20] Our results provide further insight into CZ silicon crystal growth process. Our work also represents a significant extension of cleaving wall technique to a nonpairwise additive potential. In what follows, we describe the details of our computational procedure.

The cleaving wall method calculates γ as the reversible work per unit area of forming a crystal-melt interface starting from the separate bulk phases.[17–19] To impose cleaving potential (CP) on the system, we employed cleaving walls made up of two ideal crystal layers with the same orientation as that of the interface being studied.[18,19] The total CP employed in our method is given as

$$\Psi = \sum_{i,j} \psi(r_{ij}) + \sum_{i,j<k} h(r_{ij}, r_{ik}, \theta_{jik}), \qquad (1)$$

where i represents a system particle and j and k are wall particles and r_{ij} is the distance between particle i and j. The functional form of ψ is derived from the repulsive part of the two-body term of the SW potential,

$$\psi(r) = \begin{cases} A(Br^{-p} - r^{-q})e^{[(r-a)^{-1}]} + \epsilon, & r < 2^{1/6}\sigma \\ 0, & r \geqslant 2^{1/6}\sigma. \end{cases} \qquad (2)$$

The parameters A, B, p, q, a, ϵ, and σ are given elsewhere.[16] To reduce the discontinuity in the first derivative of the CP at the cleaving plane, we modified the two-body term in Eq. (1) in the same manner as given in Ref. 19. The function h is the same as in the three-body term of the SW potential.[16] It should be noted that we only used a part of the three-body term in which a single system particle interacts with two wall particles. The other part in which two system particles interact with a single wall particle was not included, since the resulting CP is discontinuous at the cleaving plane, and with which the Nose–Hoover Hamiltonian would not be conserved during the molecular dynamics (MD) simulation.

The cleaving wall method was implemented by thermodynamic integration[18,19] (TDI) and the Bennett acceptance ratio (BAR) techniques.[21,22] We computed γ at the melting point of silicon SW potential, i.e., at $T_m^* = 0.0667$ and $P^* = 0.0$, as reported in Ref. 23 (quantities with a superscript * are dimensionless). In TDI process, we performed MD simulations along the reversible path with a time step of $\Delta t^* = 0.005$ (i.e., 0.38 fs) using Nose–Hoover thermostat. The expressions for potential energy and reversible work for the four stages are the same as given in Ref. 19. We first attempted to reproduce the TDI result for the Lennard–Jones (LJ) potential and found the results in agreement with those in the literature[19] (within error bars) for γ_{111} and γ_{100}. We next applied the TDI method to SW silicon in the four-step procedure, as described below.

In steps 1 and 2, bulk solid and liquid phases are respectively cleaved by decreasing the distance zw between the wall and the cleaving plane. The hysteresis observed in step 1 due to center of mass motion of the crystal phase,[19] could be sufficiently reduced by performing longer simulations for (100) and (110) orientations. However, for (111) orientation, the hysteresis was substantial even with longer simulations and hence we employed the BAR method[21,22] (see below). This method appears to be effective in eliminating the hysteresis, as repeated (independent) runs yielded consistent results. In step 2, we found some hysteresis due to ordering transition as in previous studies.[9] This was more pronounced for (110) orientation. Hence, for this orientation we performed the step at a higher temperature of $T = 1.15T_m$, i.e., away from coexistence conditions. A similar computational procedure was used by Davidchack and Laird[9] and more recently by Handel *et al.*[20] The initial position of the wall was $zw_i^* = 1.8$, while the final position was $zw_f^* = 0.35$, 0.75, and 0.50 for (100), (111), and (110) orientations, respectively.

[a)]New at Department of Chemical Engineering, Indian Institute of Technology, Kanpur, India
[b)]Electronic mail: xczeng@phase2.unl.edu.

 © 2008 American Institute of Physics

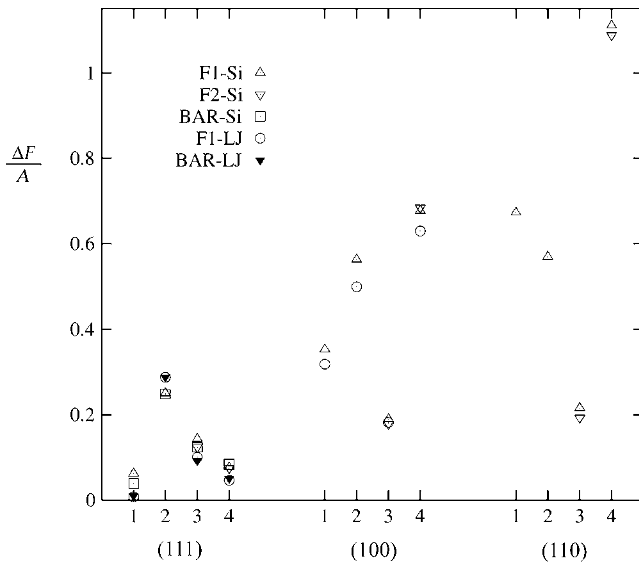

FIG. 1. Comparison of reversible work per unit area ($\Delta F/A$) for individual steps. For step 4, negative of the reversible work is shown for convenience. The units of $\Delta F/A$ are ϵ/σ^2 for LJ interface and J/m^2 for Si interfaces. Forward path 1 (F1) and forward path (F2) are TDI paths and differ only in steps 3 and 4.

In step 3, the cleaved crystal and liquid systems are combined in a reversible manner. We first examined this step at $T=T_m$, as in previous studies.[9,19] We name this as forward path 1 (F1). However, we found that there was a significant hysteresis in the region from $\lambda=0$ to 0.4 (λ is an integration parameter). This is due to the formation of metastable crystalline regions in the liquid phase near the cleaving planes. This phenomena was also observed in earlier studies[9,19] in LJ and soft-sphere systems. However, in the case of SW potential, it is more pronounced because of longer range of SW potential compared to a cut-and-shifted LJ potential. To eliminate this hysteresis, we performed the integration from $\lambda=0$ to 0.4 away from coexistence, i.e., at a higher temperature of $T=1.15T_m$. While from $\lambda=0.4$ to 1.0, the integration was performed at $T=T_m$. We call this as forward path 2 (F2). Even in this case, we found that hysteresis was persistent, although to a lesser extent. However, we found that the γ values obtained using F1 and F2 for the three orientations closely agreed (see Fig. 1). This agreement seems unlikely unless both F1 and F2 paths are reversible. Hence, we present results based only on forward paths F1 and F2, and the error estimates reported in Table I take into account the difference in the two results. A further verification of reversibility of TDI paths was carried out by comparison with the BAR method, as discussed below.

TABLE I. The system size and the interfacial free energy for each interface. The same cell size is used for the crystal and the liquid phase. The unit cell length is calculated as $a=(8/\rho_C)^{1/3}$, where ρ_C is the equilibrium density of the crystal. The value of γ in the last column is an average of the results from different methods, as reported in Fig. 1. The numbers in parenthesis are an estimated error in the last digit(s) shown.

Interface	Cell dimensions	N_C	N_L	$\gamma(J/m^2)$
Si(111)	$3\sqrt{2}a\times 3\sqrt{1.5}a\times 14\sqrt{3}a$	3024	3256	0.34(2)
Si(100)	$5a\times 5a\times 20a$	4000	4307	0.42(2)
Si(110)	$4a\times 3\sqrt{2}a\times 19\sqrt{z}a$	3648	3928	0.35(3)

In step 4, the external potential is gradually removed by increasing zw. Here also it is difficult to verify the reversibility of the path by the conventional method, i.e., comparing forward and backward runs. The reason is that the two liquid-solid interfaces can shift during the simulation by simultaneous melting and freezing, in the absence of the CP.[19] Hence, during the reverse path it is very difficult to place the cleaving plane such that its position coincides with crystal-melt interface in the same manner as in the forward path. To circumvent this difficulty, we again considered two forward paths F1 and F2, as defined in step 3. The results of the two paths matched closely, as shown in Fig. 1.

To further support our results, we also employed BAR method[21,22] to compute γ for Si(111) interface. We first verified our implementation of BAR method by calculating γ^* for LJ(111) crystal-melt interface. The reversible work obtained for individual steps agrees well with TDI method (Fig. 1). While the value of γ^* from BAR method [0.339(2)] slightly differs from TDI method [0.349(6)], it is sufficiently close. We then applied BAR method to Si(111) interface and found reasonably good agreement with TDI method, as shown in Fig. 1. It should be noted that the two methods calculate Helmholtz free energy difference ΔF differently. In BAR method, ΔF is calculated as a ratio of canonical ensemble averages of a properly chosen weight function,[21] whereas in TDI method, the estimate of ΔF is based on the derivative of the free energy with respect to a parameter that defines the reversible path. In TDI method, the entire path must be reversible, i.e., all the states along the path must be stable equilibrium states, whereas in BAR method only the end states must be stable equilibrium states and the result is independent of the path connecting the two states.[22] The agreement between the two independent methods affirms that TDI path is reversible for SW Si(111) interface. We expect that the same conclusion will hold for other orientations as TDI path is qualitatively the same.

From Table I, we find that $\gamma_{100} > \gamma_{111}, \gamma_{110}$. The orientationally averaged value $\bar{\gamma}$ (Refs. 19 and 24) was found to be $0.37(3)$ J/m^2, which compares fairly well with earlier results of $0.41-0.43$ J/m^2 obtained from the superheating-undercooling method for SW potential.[15] Note also that $\bar{\gamma}$ is in reasonable agreement with reported experimental results $\gamma \sim 0.34-0.45$ J/m^2 (obtained based on the classical theory of nucleation).[10–12]

It is important to probe whether empirical SW potential we employed is realistic. For silicon, more than 16 empirical potentials have been proposed.[25] However, we chose SW potential for the following reasons: This potential predicts a melting temperature of silicon close to the experimental value[23] and it has been shown that SW potential describes liquid Si surface[26] and crystalline Si(100) surface farely well[25,27] and that it also exhibits (111) faceting on Si(100)-melt interface, as observed experimentally.[4,5] Thus, the results we obtained based on SW potential are expected to be fairly accurate. Note also that SW potential has been used in a number of studies related to crystal-melt interface.[2,5,28] Nonetheless, it will be necessary to study the dependence of γ on the model potential[29] by employing several different potentials of silicon [e.g., Tersoff-89 (Ref. 30)] and this task will be undertaken as a future work.

Our results are consistent with experimental observations noted earlier. Since γ_{111} is substantially smaller (by about 20%) than γ_{100}, the equilibrium Si(100)-melt interface

develops (111) facets in order to lower the free energy, thus resulting in a rough interface. On the other hand, Si(111)-melt interface remains smooth and sharp (flat) due to its higher stability. Also, our calculations indicate that higher undercooling at Si(111)-melt interface during CZ growth process could be due to its lower surface free energy compared with other orientations. It is to be noted that in a supercooled liquid, γ serves to counteract the effect of free energy difference between solid and liquid phases.[20] Thus, lower γ means that more driving force (supercooling) required for CZ crystal growth.

In conclusion, the anisotropy of interfacial free energy for Si is resolved using the SW potential. Our results are consistent with experimental observations that underlying anisotropy in γ plays a crucial role in CZ crystal growth process. The qualitative trend in anisotropy we observed could also be relevant for other diamond structured materials such as germanium which is often modeled using SW potential.[31] On the computational front, we have extended cleaving wall method to nonpairwise additive potential and this opens up the possibility of studying other materials modeled through empirical many-body potentials.

We thank Dr. J. R. Morris for valuable discussions. This study was supported by grants from DOE (DE-FG02-04ER46164), NSF, the Nebraska Research Initiative, and by the Research Computing Facility at UNL.

[1] G. Muller, J. J. Metois, and P. Rudolph, *Crystal Growth–From Fundamentals to Technology* (Elsevier, Amsterdam, 2004).
[2] F. F. Abraham and J. Q. Broughton, Phys. Rev. Lett. **56**, 734 (1986).
[3] K. M. Beatty and K. A. Jackson, J. Cryst. Growth **211**, 13 (2000).
[4] K. Fujiwara, K. Nakajima, T. Ujihara, N. Usami, G. Sazaki, H. Hasegawa, S. Mizoguchi, and K. Nakajima, J. Cryst. Growth **243**, 275 (2002).
[5] U. Landmann, W. D. Luedtke, R. N. Barnett, C. L. Cleveland, M. W. Ribarsky, E. Arnold, S. Ramesh, H. Baumgart, A. Martinez, and B. Khan, Phys. Rev. Lett. **56**, 155 (1986).
[6] D. J. Eaglesham, A. E. White, L. C. Feldman, N. Moriya, and D. C. Jacobson, Phys. Rev. Lett. **70**, 1643 (1993).
[7] R. E. Napolitano, S. Liu, and R. Trivedi, Interface Sci. **10**, 217 (2002).
[8] J. R. Morris, Z. Y. Lu, Y. Y. Ye, and K. M. Ho, Interface Sci. **10**, 143 (2002).
[9] B. B. Laird and R. L. Davidchack, J. Phys. Chem. B **109**, 17802 (2005).
[10] S. R. Stiffler, M. O. Thompson, and P. S. Peercy, Phys. Rev. Lett. **60**, 2519 (1988).
[11] R. P. Liu, T. Volkmann, and D. M. Herlach, Acta Mater. **49**, 439 (2001).
[12] Y. Shao and F. Spaepen, J. Appl. Phys. **79**, 2981 (1996).
[13] Z. Jian, K. Kuribayashi, W. Jie, and F. Chang, Acta Mater. **54**, 3327 (2006).
[14] X. C. Zeng and D. Stroud, J. Phys.: Condens. Matter **1**, 1779 (1989).
[15] Y. W. Tang, J. Wang, and X. C. Zeng, J. Chem. Phys. **124**, 236103 (2006).
[16] F. H. Stillinger and T. A. Weber, Phys. Rev. B **31**, 5262 (1985).
[17] J. Q. Broughton and G. H. Gilmer, J. Chem. Phys. **84**, 5759 (1986).
[18] R. L. Davidchack and B. B. Laird, Phys. Rev. Lett. **85**, 4751 (2000).
[19] R. L. Davidchack and B. B. Laird, J. Chem. Phys. **118**, 7651 (2003).
[20] R. Handel, R. L. Davidchack, J. Anwar, and A. Brukhno, Phys. Rev. Lett. **100**, 036104 (2008).
[21] C. H. Bennett, J. Comput. Phys. **22**, 245 (1976).
[22] Y. Mu and X. Song, J. Chem. Phys. **124**, 034712 (2006).
[23] S. Yoo, X. C. Zeng, and J. R. Morris, J. Chem. Phys. **120**, 1654 (2004).
[24] X. Feng and B. B. Laird, J. Chem. Phys. **124**, 044707 (2006).
[25] H. Balamanc, T. Halicioglu, and W. A. Tiller, Phys. Rev. B **46**, 2250 (1992).
[26] Z. Q. Wang and D. Stroud, Phys. Rev. B **38**, 1384 (1988).
[27] L. Nurminen, F. Tavazza, D. P. Landau, A. Kuronen, and K. Kaski, Phys. Rev. B **67**, 035405 (2003).
[28] D. Buta, M. Asta, and J. J. Hoyt, J. Chem. Phys. **127**, 074703 (2007).
[29] J. R. Morris, M. I. Mendelev, and D. J. Srojovitz, J. Non-Cryst. Solids **353**, 3565 (2007).
[30] J. Tersoff, Phys. Rev. B **39**, 5566 (1989).
[31] P. Spiewak, M. Muzyk, K. J. Kurzydlowski, J. Vanhellemont, K. Mlynarczyk, P. Wabinski, and I. Romandic, J. Cryst. Growth **303**, 12 (2007).